



Aspergillus nidulans *hypB* encodes a Sec7-domain protein important for hyphal morphogenesis

Yi Yang^{a,1}, Amira M. El-Ganiny^a, Geoffrey E. Bray^{a,2}, David A.R. Sanders^b,
Susan G.W. Kaminskyj^{a,*}

^a Department of Biology, University of Saskatchewan, 112 Science Place, Saskatoon, Sask., Canada S7N 5E2

^b Department of Chemistry, University of Saskatchewan, 110 Science Place, Saskatoon, Sask., Canada S7N 5C9

Received 21 September 2007; accepted 19 November 2007

Abstract

Aspergillus nidulans strains containing the *hypB5* temperature sensitive allele have a restrictive phenotype of wide, highly-branched hyphae. The *hypB* locus was cloned by phenotype complementation using a genomic plasmid library. *hypB5* is predicted gene AN6709 in the *A. nidulans* genome database, which encodes a putative Sec7 domain protein, likely to act early in COPI-mediated vesicle formation for retrograde Golgi to ER transport. The *A. nidulans hypB5* allele has a single mutation, cytosine to guanine predicted to cause a nonconservative amino acid change, alanine to proline, in a conserved helix adjacent to the Sec7p nucleotide binding site. This would likely reduce the stability of a highly conserved loop important for nucleotide binding, and is consistent with temperature sensitivity of *hypB5* strains. Deletion of AN6709 showed that *hypB^{Sec7}* was not essential. AN6709Δ hyphae resembled the *hypB5* restrictive phenotype. As has been shown previously for *hypA1* mutants, shifting established *hypB5* mutant hyphae from a growth temperature of 28–42 °C caused septation in and death of tip cells and growth activation of basal cells.

© 2007 Elsevier Inc. All rights reserved.

Keywords: ARF; *Aspergillus nidulans*; GEF; *hypB5*; Hyphal morphogenesis; COPI; Membrane trafficking; Secretion; Sec7p

1. Introduction

Fungal tip growth requires targeted secretion of vesicles that contain wall synthetic materials (Bartnicki-Garcia, 2002), most of which are synthesized by the endoplasmic reticulum (ER) then modified and/or packaged prior to secretion. Fungal Golgi equivalents (also called dictyosomes) have analogous function to animal Golgi complexes but differ in appearance, since they are single pleiomorphic

cisternae (Kaminskyj and Boire, 2004; Kurtz et al., 1994). We will refer to them as fungal Golgi. Endomembrane vesicle trafficking is controlled by a suite of gene products, some of which are common to all eukaryotes, whereas others are restricted to fungi, or even to filamentous fungi (Harris and Momany, 2004; Harris et al., 2005; Harris, 2006; Virag and Harris, 2006).

Mutant analysis is a powerful method for identifying genes whose products are required for wildtype hyphal morphogenesis. In *Aspergillus nidulans*, analysis of temperature sensitive morphological mutants has identified genes that affect cell polarization (Harris et al., 1999), actin cytoskeletal function (Harris et al., 1999; Sharpless and Harris, 2002), wall maturation (Hill et al., 2006; Momany et al., 1999), vesicle formation (Shaw et al., 2002), endomembrane transport (Shi et al., 2004), and other events (Harris et al., 1994; Harris et al., 1999; Lin et al., 2003; Osheroev et al., 2000).

* Corresponding author. Fax: +1 306 966 4461.

E-mail address: susan.kaminskyj@usask.ca (S.G.W. Kaminskyj).

¹ Present address: Department of Oral Biological and Medical Sciences, Faculty of Dentistry, University of British Columbia, 398-2199 Wesbrook Mall, Vancouver, BC, Canada V6T 1Z3.

² Present address: Department of Anatomy and Cell Biology, College of Medicine, University of Saskatchewan, 107 Wiggins Road, Saskatoon, Sask., Canada S7N 5E5.

At their restrictive temperature, *A. nidulans* hypercellular mutants have wide, slowgrowing hyphae with short basal cells (Kaminskyj and Hamer, 1998). Shi et al. (2004) described the molecular cloning of *hypA*, whose *S. cerevisiae* homologue, *TRSI20* is a regulatory component of the TRAPP II (transport protein particle)³ complex involved in diverse Golgi-related functions (Cai et al., 2005; Guo et al., 2000; Kim et al., 2006). Here, we report the molecular cloning of *A. nidulans hypB*, by complementing the recessive *hypB5* temperature sensitive phenotype using the Oshero and May (2000) genomic plasmid library. HypB is encoded by the predicted protein AN6709.4 in the *A. nidulans* genome database. AN6709 contains a region with high identity to *Saccharomyces cerevisiae SEC7*.

2. Materials and methods

Biological materials and primers are given in Table 1. Chemicals were reagent grade and were purchased from VWR (www.vwrcanlab.ca) or Sigma (www.sigmaaldrich.ca) unless stated otherwise. Water was 18 M Ω deionized (www.labwater.com), and sterilized as appropriate. *A. nidulans* strains were grown in complete medium (CM) with nutritional supplements as required (Kaminskyj, 2001). *Escherichia coli* strains were grown in Luria Bertani (LB) broth or agar, supplemented with antibiotics for selectable markers.

Statistical analyses used Statview SE + Graphics v1.02. Values are presented as means \pm standard error. Graphs were prepared with Cricket Graph (1.3.1). Images were prepared with Adobe Photoshop 7.0.

2.1. Microscopical methods

For cell morphometry, freshly harvested *A. nidulans* conidia were germinated and grown on single 22 mm \times 22 mm coverslips in 60 mm diameter Petri dishes containing 5 mL liquid CM. Germlings were grown for 20 h at 28 $^{\circ}$ C or 42 $^{\circ}$ C, or for 14 h at 28 $^{\circ}$ C followed by up to 3 h at 42 $^{\circ}$ C. Inocula were 50,000 spores/mL for cultures grown at 42 $^{\circ}$ C, and 5000/mL for those grown at 28.

For cell morphometry, samples were fixed and stained with Calcofluor to visualize walls and Hoechst 33258 to visualize nuclei as described in Kaminskyj and Hamer (1998). Morphometric methods are described in Kaminskyj and Hamer (1998). Hyphal width was measured at septa, typically 30 per strain and growth condition. Basal cell length was measured between adjacent septa. Nuclei per basal cell were counted in the same cells. Light microscopy used a Zeiss Axioplan microscope, 63 \times NA 1.4 Plan Apo-

³ Abbreviations used: ARF, ADP-ribosylation factor; ARNO, ADP-ribosylation nucleotide binding site opener; COG, conserved oligomeric golgi; COPI, coat protein complex I; COPII, coat protein complex II; GEF, guanine nucleotide exchange factor; TRAPP, transport protein particle.

chromat oil immersion objective and epifluorescence illumination using a G365 excitation filter, FT395 dichroic mirror, and LP420 emission filter. Images were captured on Kodak TMax 3200 film, or with a Sensys cooled CCD (www.roper.com) driven by Micromanager software. Cell membrane integrity was assessed with transmitted light as ability to exclude toluidine blue (Kaminskyj, 2000). Confocal imaging used a Zeiss META510 confocal microscope with a 405 diode at 20% power, and a 420–480 nm emission filter. Confocal fluorescent and transmitted images were collected simultaneously.

For endomembrane array staining, 0.5 μ g FM4-64 (probes.invitrogen.com) was dissolved in 100 μ L ethanol. Just prior to use, 4 μ L of this stock was diluted into 100 μ L liquid CM for a final FM4-64 concentration of 20 pg/ μ L. Freshly harvested *A. nidulans* conidia were germinated and grown on coverslips in liquid CM at 28 $^{\circ}$ C or 42 $^{\circ}$ C for 16 h. For staining, the CM was drained, the coverslip was placed germling-side up in the lid, and incubated for 30 min at the growth temperature in 50 μ L FM4-64 staining solution (held in place by surface tension), using the bottom half of the Petri dish to create a moist chamber. After 30 min, the coverslip with stained germlings was flooded with 2 mL of pre-warmed CM liquid, and incubation was continued for at least 90 min prior to examination. Cells were examined using widefield fluorescence, using BP546 excitation, a FT580 dichroic, and LP 590 emission filters.

2.2. Molecular methods

Aspergillus nidulans transformation was described in Shi et al. (2004). *A. nidulans* strain ASK166 was transformed with 1 μ g of the *A. nidulans* pRG3AMA1 NotI genomic library (Oshero and May, 2000), and selected for pyrimidine prototrophy. Transformants were incubated at 28 $^{\circ}$ C for 18 h before testing for phenotype complementation at 42 $^{\circ}$ C. Genomic DNA was extracted from a transformant that had produced a wildtype colony at 42 $^{\circ}$ C (named AYY1), and used to transform *E. coli* strain XL1Blue (tet^R) to ampicillin resistance. This generated pYY1, which had a 16 kb plasmid insert. Restriction fragments from pYY1 were cotransformed with plasmid ARp1-NCpyr4⁺ into the *hypB5* strain ASK166. Transformants were selected as described above. The smallest fragment that could repair the *hypB5* defect, a 5 kb KpnI fragment, was subcloned into pBluescript^{chlorR}, selected on LB containing chloramphenicol, and named pYY2. Subsequent experiments to study this sequence used DNA cotransformed with an AMA1 plasmid containing *Neurospora crassa pyr4*⁺ as a selectable marker (Shi et al., 2004), and selected as described previously.

Transposon disruption by Tn1000 insertion (Strathmann et al., 1991) into pYY2 was accomplished by mating (Shi et al., 2004) the pYY2^{chlorR} strain with DH5 α ^{rifR}. Mated colonies were selected on LB containing chloramphenicol and rifampicin. A set of pYY2 strains with

Table 1
Biological materials used in this study

<i>Aspergillus nidulans</i>	
A28 ^a	<i>biA1, pabaA6; veA1</i>
A1145 ^a	<i>pyrG89, pyroA4, nkuAΔ, veA1</i>
AKS4 ^b	<i>hypA1, hypB5, biA1, pabaA6; pyro A4; chaA1, veA1</i>
ASK80 ^{a,c}	<i>hypB5, pabaA6; chaA1, veA1</i>
ASK166 ^b	<i>hypB5, pyrG89; wA2; veA1</i>
AYY1 ^b	ASK166 complemented with pRG3-AMA1, wA2; <i>veA1</i>
AN6709Δ ^b	AN6709::AFpyrG, <i>pyrG89, pyroA4, nkuAΔ, veA1</i>
<i>Escherichia coli</i>	
XL1-Blue ^b	tet ^R
DH5α ^{fif Rb}	A spontaneous mutant of DH5α, selected on rifampicin
Plasmids	
AO81 ^{a,c}	S-TAG <i>Aspergillus fumigatus pyrG</i> , kan ^R
ARp1-NC <i>pyr4</i> ^{+ d}	AMA1 plasmid, <i>Neurospora crassa pyr4</i> ⁺ , amp ^R
pBCSK ^{+ f}	chlor ^R
pRG3-AMA1 (NotI) ^{a,g}	<i>Aspergillus nidulans</i> genomic plasmid library, amp ^R
pYY1 ^{a,c}	16 kb pRG3-AMA1 (NotI) <i>ura4</i> ⁺ , <i>hypB5</i> complementing, amp ^R
pYY2 ^{a,c}	5 kb KpnI fragment of pYY1, <i>hypB5</i> complementing, chlor ^R
Primers (5'→3')	
GDIR	TTTCGTTCCATTGGCCCTCAAACCCC
GD1	CAACGAATTATCTCCTT
GD2	TCAATAAGTTATAACCAT
T3	AATTAACCCTCACTAAAGGG
T7	GTAATACGACTCACTATAGGGC
pYY2 2334-2351	ACAACGTAGCGTTGACCC
pYY2 3179-3160	CCAACCGTTGCGAAGACTTG
P1	AGCTGAACGATTCAAAGCC
P2	TACACTTGGAGGCGTAGTAACGT
P3	AATTGCGACTTGGACGACATTATGCAAGACTCCGTCTGGA
P4	GAGTATGCGGCAAGTCATGACTGGTTTTCTTCTTATATCCGC
P5	CTTGCAAGTATGGTTCGAAAGA
P6	TTTGTTCCCTATTCTGCCAAG
P8	CAATACCGTCCAGAAGCAATAC
Ppyrf	ATGTCGTCCAAGTCGCAATT
Ppyrr	TCATGACTTGCCGCATACTC
AN6709for	ATGGCGGAAGCTGAGAAC
AN6709rev	TCAGCGCCGCCGA

^a Fungal Genetics Stock Center (www.fgsc.net).

^b This study.

^c Kaminskyj and Hamer (1998).

^d Shi et al. (2004).

^e Yang et al. (2004).

^f Stratagene.

^g A gift of N. Osherov and G. May, University of Texas, M. D. Anderson Cancer Center.

Tn1000 insertions about 500 bp apart was identified by PCR with DGIR/T3 or DGIR/T7 primers. Primers DG1, DG2, T3, and T7 were used for sequencing the pYY2 insert. This set of insertion strains was also used to determine which part(s) of pYY2 were important for *hypB5* restrictive phenotype rescue (Hamer et al., 2001). ASK166 was co-transformed with 4 μg of individual pYY2 plasmids containing one of the panel of Tn1000 insertions used for sequencing, plus 1 μg ARp1-NC*pyr4*⁺, and tested for their ability to repair the *hypB5* mutation at 42 °C. Additional details are provided in Fig. 1.

To identify the lesion site in *hypB5*, the Sec7 coding region in pYY2 was PCR-amplified from ASK166 genomic DNA using primers pYY2 2334-2351 and pYY2 3179-3160 and *Pfx* polymerase (Invitrogen). Amplicons from three inde-

pendent, replicate PCRs were sequenced. Each showed the same mutation with respect to the wildtype pYY2 sequence, AN6709.4, which had been obtained by blast searching at www.broad.mit.edu/annotation/fungi/aspergillus/.

An *Aspergillus nidulans* strain deleted for AN6709, AN6709Δ was generated following the procedures described in Nayak et al. (2006) and Szewczyk et al. (2007), using *Aspergillus fumigatus pyrG* as a selectable marker. Transformant colonies were grown on selective medium and allowed to conidiate. These spores were germinated on selective medium to examine hyphal morphology and to generate mycelium for extracting genomic DNA. The AN6709 deletion locus was confirmed by diagnostic PCR using A1145 and AN6709Δ genomic templates. Details are provided in Fig. 2.

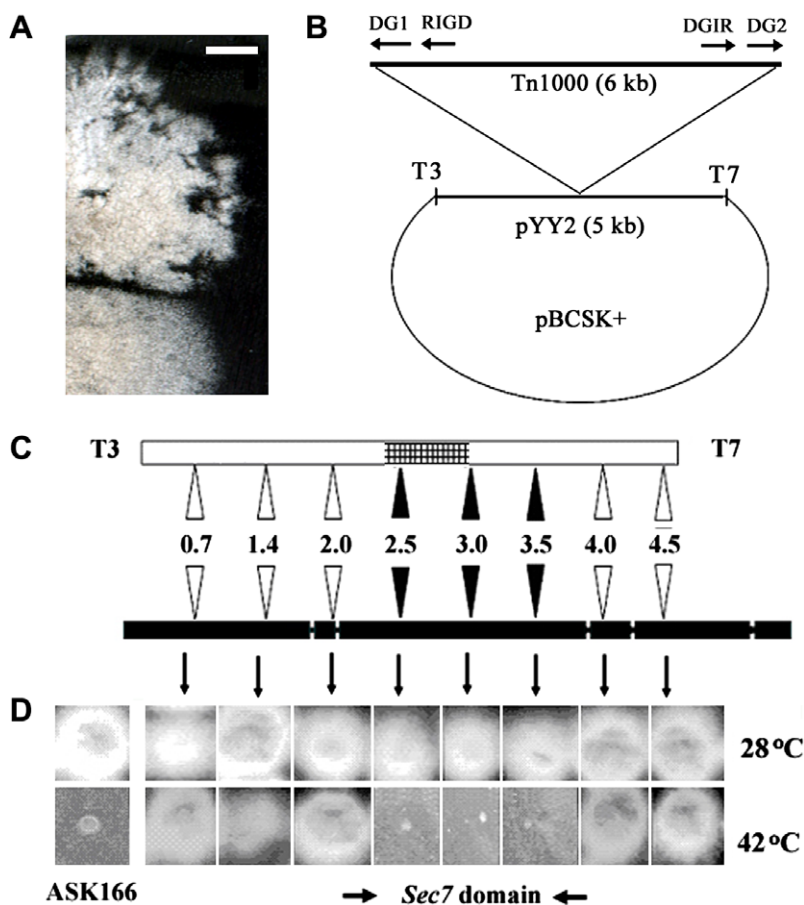


Fig. 1. Molecular analysis of *hypB*. (A) Strain *hypB5* strains transformed with pYY1 and pYY2, grown at 42 °C on medium containing pyrimidines. The pYY1 transformant (upper colony) produced sectoried colonies, indicating plasmid loss on nonselective medium. In contrast, the pYY2 transformant (lower colony) did not sector on the same medium, suggesting that phenotype rescue had been by gene repair. Bar = 5 mm. (B) A cartoon of the pYY2 plasmid, which contains a 5 kb KpnI insert in pBCSK⁺ that rescues the *hypB5* defect at 42 °C. The Tn1000 transposon was randomly inserted (see Section 2) into the pYY2 insert by mating its *E. coli* host strain with a rifampicin resistant mutant, DH5 α ^{rif^R}. Tn1000 contains a sub-terminal inverted repeat (RIGD/DGIR) and unique terminal sequences DG1 and DG2. A suite of chloramphenicol/rifampicin resistant *E. coli* strains with Tn1000 insertions spaced about 600 bp apart in pYY2 were identified by PCR amplification using DGIR and T3 or T7 primers. pYY2 was sequenced using this suite of Tn1000 insertion strains, plus T3, T7, DG1 and DG2 primers. (C) A cartoon depicting the pYY2 sequence (top: open bar, and its predicted Sec7p domain, hatched bar), the positions of the Tn1000 insertions in the panel of strains used for sequencing and for characterization (middle: in kb from the T3 end), and predicted gene AN6709 (bottom: black bar, with predicted introns shown as gaps). The predicted third exon in AN6709 has high similarity to *Saccharomyces cerevisiae* SEC7 (hatched region in the pYY2 map). Parts C and D are aligned to facilitate comparison of pYY2 and AN6709, and the effect of Tn1000 insertions into pYY2 on its ability to rescue the *hypB5* defect at 42 °C. (D) Colony phenotypes for transformants from the panel of Tn1000 insertion strains, cotransformed with ARp1-NCpyr4⁺ growing on selective medium at 28 °C and 42 °C. Three individual plasmids containing different Tn1000 insertions into the pYY2 predicted Sec7p domain (hatched region/third exon) shown in C, failed to rescue the *hypB5* defect at 42 °C shown in D, unlike five other plasmids containing Tn1000 in other parts of the pYY2 insert. Colony morphology of the ASK166 (*hypB5*, *pyrG89*, *wA2*) strain grown on medium supplemented with pyrimidines is shown for comparison.

3. Results

3.1. *Aspergillus nidulans hypB5* encodes a Sec7p-encoding sequence

The *hypB* locus was cloned by complementing the *hypB5* temperature sensitive phenotype using the *A. nidulans* pRG3-AMA1 genomic library (Osheroev and May, 2000). A transformant was chosen for its wildtype colony morphology at the *hypB5* restrictive temperature, and named AYY1. AYY1 colonies sectoried on medium containing pyrimidines when grown at the *hypB5*-restrictive temperature (upper colony in Fig. 1A), showing that the growth

was plasmid-dependent. The complementing plasmid was rescued by transforming *E. coli* strain XL1-Blue to ampicillin resistance with DNA isolated from AYY1, and named pYY1. A 5 kb KpnI subclone of pYY1, called pYY2 could rescue the *hypB5* defect, producing colonies with a wildtype hyphal morphology at 28 °C and 42 °C. Unlike the pYY1-complemented strain AYY1, pYY2-rescued *hypB5* colonies did not sector on non-selective medium (lower colony in Fig. 1A), suggesting there had been gene repair rather than complementation.

pYY2 was sequenced using a panel of Tn1000 insertion mutants (Fig. 1B and C). The pYY2 insert sequence begins 34 bp upstream of the predicted translation start of

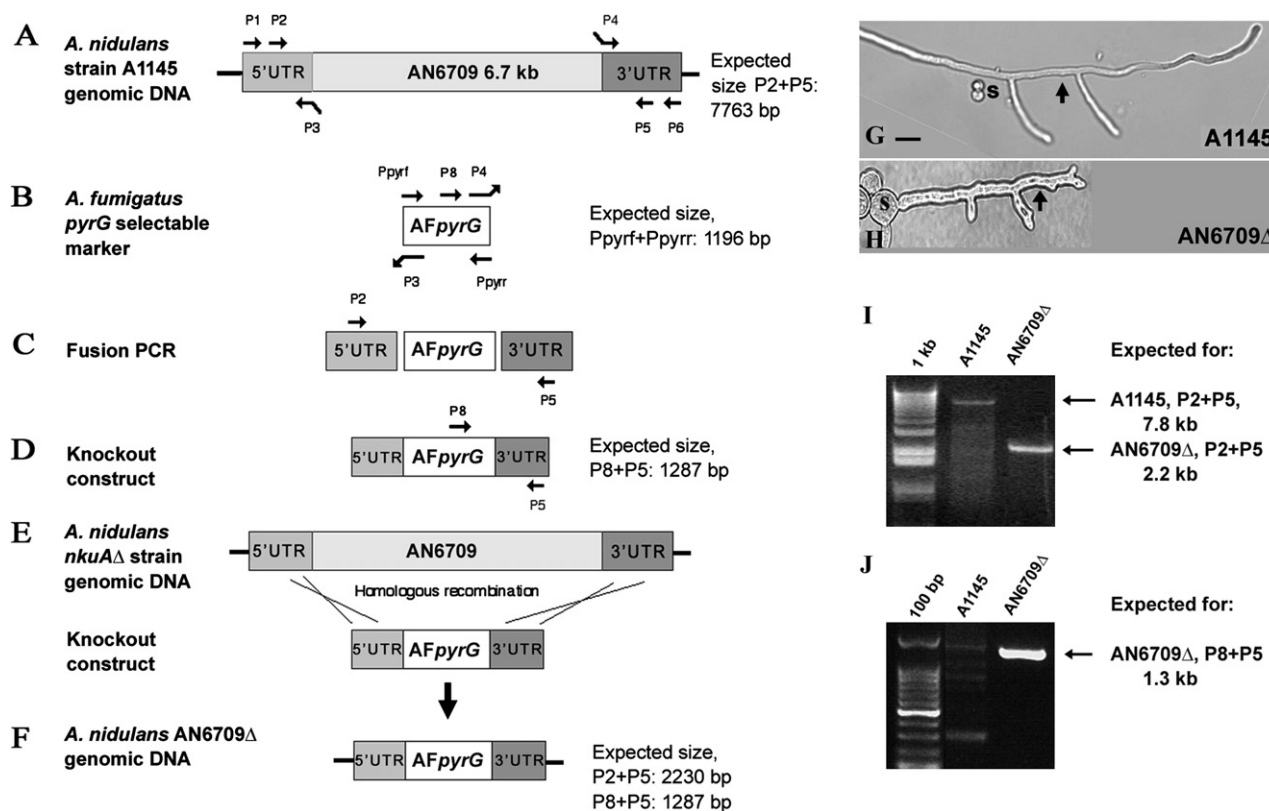


Fig. 2. Deletion of *Aspergillus nidulans* AN6709. (A) The 5' and 3' untranslated regions (5'UTR and 3'UTR, respectively) flanking AN6709 were amplified using P1 + P3 and P4 + P6, respectively, from A1145 (*nkuAΔ*, *pyrG*) genomic DNA template. Primer sequences are provided in Table 1. P3 and P4 are bridging primers between the flanking regions and the selectable marker. (B) The selectable marker, *A. fumigatus pyrG*, was amplified from plasmid AO81 with Ppyrf and Ppyr. (C) Fusion PCR (semi-nested, with primers P2 + P5) using mixed template (5'UTR, AFpyrG, 3'UTR), with complementary ends generated the bridging primers P3 and P4, created (D) the linear knockout construct with 500 bp AN6709-flanking regions. (E) A1145 protoplasts were transformed with the knockout construct. Homologous recombination between the flanking regions replaced AN6709 with AFpyrG. Putative AN6709 knockout transformants were selected on medium lacking pyrimidines. (F) Predicted AN6709Δ genomic DNA. (G, H) Morphology of A1145 and AN6709Δ on medium lacking pyrimidines. Arrows indicate the most apical septum. Bar in G = 10 μm, for both. See also Fig. 4. (I) PCR using primers P2 + P5 for genomic DNA template isolated from A1145 and AN6709Δ. Both strains amplified the band sizes expected, described also in parts A and F. (J) PCR using the same genomic DNA templates as in I, with P8 + P5 primers. The A1145 template amplified a few weak bands, whereas the AN6709Δ template amplified a single strong band of the expected size (see also the cartoon in part F), indicating that the AN6709Δ strain contains *A. fumigatus pyrG* at the AN6709 locus.

AN6709, and was identical to that of AN6709 for the first 4707 bp. AN6709 is predicted to encode a peptide of 1999 amino acids (estimated molecular weight 219 kDa), including a putative Sec7-domain that is homologous to *Saccharomyces cerevisiae SEC7* (AAB04031). The pYY2 sequence was deposited in GenBank as AY261780. Consistent with the sequence identity between pYY2 and the majority of the AN6709 sequence, the *hypB5* defect was rescued by PCR-amplified wildtype AN6709 when it was co-transformed with ARp1-NCpyr4⁺ into ASK166.

AN6709 is predicted to have five introns, with exon 3 encoding a Sec7p domain that is predicted to be 190 amino acids long. Sec7p domains are highly conserved from yeasts to mammals (Cox et al., 2004). The AN6709 predicted Sec7p domain is 81% identical to that of *S. cerevisiae SEC7*, with a secondary structure predicted to be 61% alpha helix and 39% coil (www.bork.emblheidelberg.de/cgi/sscp_serv.pl).

The panel of pYY2 Tn1000 insertion strains used in sequencing pYY2 was also used for functional analysis

since the 6 kb Tn1000 transposon is expected to disrupt gene function if inserted into an essential sequence (Hamer et al., 2001). Plasmid DNA from each member of the pYY2 Tn1000 insertion panel was co-transformed with ARp1-NCpyr4⁺ into ASK166, selected on medium lacking pyrimidines, and tested for phenotype rescue at 42 °C. pYY2 strains with a Tn1000 insertion near the putative Sec7p domain coding region (hatched box in Fig. 1C) did not rescue the *hypB5* phenotype (black triangles in Fig. 1C), despite being transformed to pyrimidine prototrophy (Fig. 1D), unlike Tn1000 insertions elsewhere in pYY2 (white triangles).

3.2. Deletion analysis

To determine if AN6709 was essential, it was replaced with *A. fumigatus pyrG* in the *nkuAΔ* strain A1145. The deletion cassette was constructed and transformed into A1145 protoplasts (Fig. 2A–F). Transformants were

selected on medium lacking pyrimidines, and allowed to conidiate. These AN6709 Δ conidia were able to germinate on selective medium (Fig. 2G and H) but their hyphal morphology was distinctly different from the A1145 parent (Fig. 2I), being almost twofold wider, and having near-apical branches and septa. Genomic DNA extracted from A1145 and AN6709 Δ mycelium was used as template for diagnostic PCR. Primers P2 + P5 amplified a major band at 7.8 kb for A1145, the expected size for AN6709 plus flanking regions, and a 2.2 kb fragment from AN6709 Δ (cf. Fig. 2A, F, I). Primer P8 was designed against a sequence in the middle of the AF $pyrG$. PCR using P8 + P5 amplified a single, strong 1.3 kb band from AN6709 Δ genomic DNA (cf. Fig. 2D and J), but not from A1145, indicating that gene replacement had occurred at the AN6709 locus. Thus, AN6709 is not essential.

3.3. Analysis of the *hypB* Sec7p domain

The crystal structure of the human Arf nucleotide binding opener (ARNO) Sec7p domain structure has been solved (Cherfils et al., 1998). The Sec7p domain from pYY2 was threaded onto the ARNO (PDB: IPVB) structure using Modeller (Sali and Blundell, 1993). There is excellent agreement between the AN6709 predicted Sec7p domain and the known crystal structure of ARNO (Fig. 3A). Sec7p domains contain 10 alpha helices, designated A–J, of which F–H (Fig. 3B) are highly conserved. The loop between helices F and G is important for nucleotide binding (Mosessoova et al., 1998).

Genomic DNA from *A. nidulans* *hypB5* strain ASK166 and the morphological wildtype strain A28 spanning the predicted Sec7p domain was amplified by PCR, and sequenced. Comparison of DNA sequences from three independent ASK166-derived amplicons with the AN6709 sequence revealed a single basepair substitution (cytosine

to guanine) resulting in a nonconservative amino acid substitution, alanine to proline (A815P) in predicted AN6709 Sec7p domain helix F (arrow in Fig. 3B). Alanine at this position is conserved across fungi and metazoans (Fig. 3C).

3.4. The *hypB5* restrictive phenotype

The *hypB5* temperature sensitive mutation affects cell polarity establishment and maintenance. Like their morphological wildtype A28 mutagenesis parent, strains containing the *hypB5* temperature sensitive morphogenesis allele had a wildtype phenotype following overnight growth at 28 °C (Fig. 4A), whereas following growth at 42 °C the hyphae were significantly wider and had more closely spaced septa (Table 2; Fig. 4B). The *hypB5*-complemented strain, AYY1 resembled wildtype at the *hypB5* restrictive temperature (Fig. 4C). The AN6709 Δ strain grown at the *hypB5* permissive temperature had wide, sometimes uneven-diameter hyphae (Fig. 2G and Fig. 4D, E) reminiscent of the *hypB5* restrictive phenotype. At the *hypB5* restrictive temperature, AN6709 Δ cells had more abundant nuclei (Fig. 4E) than at the permissive temperature. At both temperatures, AN6709 Δ lateral branching resembled the *hypB5* restrictive phenotype (Fig. 2H and Fig. 4D, E), unlike wildtype strains (Fig. 2G, Fig. 4A). AYY1 had a wildtype phenotype at the *hypB5* restrictive temperature, whereas the AN6709 Δ strain resembled the *hypB5* restrictive phenotype but at the *hypB5* permissive temperature.

Endomembrane arrays were characterized using FM4-64 in the *hypB5* strain ASK80 following overnight growth at 28 °C and 42 °C. FM4-64 is taken up by endocytosis and after sufficiently long incubation (at least 45 min) reveals endomembrane arrays in the secretory pathway. In the *hypB5* permissive phenotype, FM4-64 is intense near the hyphal tip, and in subapical regions localizes to a reticulate

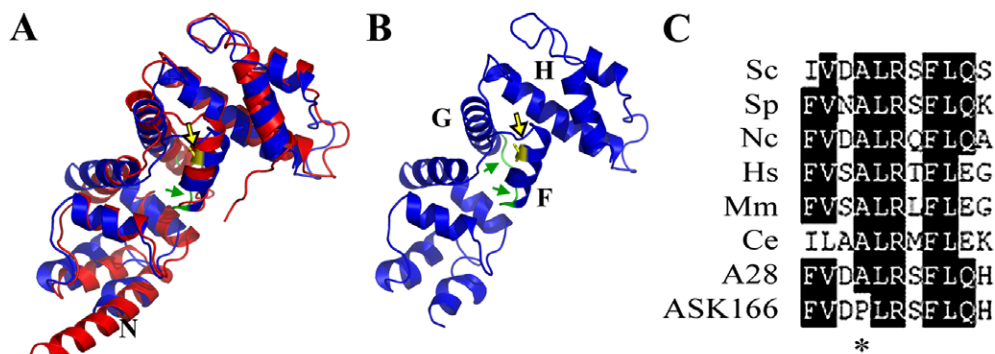


Fig. 3. The ARNO Sec7p domain crystal structure, the AN6709 Sec7p predicted structure, and the site of the lesion in *hypB5*. (A) The AN6709 Sec7p domain (blue) threaded onto the crystal structure of the human ADP ribosylation nucleotide opener, ARNO (red) using Modeller. (B) The AN6709 predicted Sec7p structure, showing the alpha helices (F, G, H) that surround the active site in *Saccharomyces cerevisiae* Sec7p. The F–G loop (green; indicated with a green arrow) is the most highly conserved motif. The site of the lesion in *hypB5*, A815P (yellow, indicated with a yellow arrow) on helix F is shown as the wildtype alanine. (C) Alignments of amino acid sequences for helix F from *Saccharomyces cerevisiae* (Sc, AAB04031), *Schizosaccharomyces pombe* (Sp, CAB55182), *Neurospora crassa* (Nc, XP962785), *Homo sapiens* (Hs, AAH50449), *Mus musculus* (Mm, BAD90330), *Caenorhabditis elegans* (Ce, CAA21704), and for *Aspergillus nidulans* (An, AY261780) strains A28 and ASK166. The asterisk indicates the position of the A815P mutation in ASK166 that corresponds to a conserved alanine in the A28 mutagenesis parent and the other species.

array (Fig. 5A). In contrast in the *hypB5* restrictive phenotype, FM4-64 staining is reduced near the hyphal apex (Fig. 5B), with predominant localization in punctate near-apical arrays and reticulate basal arrays.

When *hypB5* cells were grown overnight at 28 °C and then shifted to 42 °C for 3 h, the nuclei in tip cell compart-

ments condensed and fragmented, triggered tip cell septation, and then the tip cells died (Fig. 4F). This is reminiscent of the growth upshift phenotype shown by *hypA1* cells (Kaminskyj and Hamer, 1998; Kaminskyj, 2000) however, *hypA* and *hypB* are independent loci. A *hypA1*, *hypB5* double mutant (AKS4) grows slowly at 28 °C, is morphologically compromised above 35 °C, and has a tip cell septation and death phenotype like its parents (not shown) following growth temperature upshift.

Events during the development of the *hypB5* upshift phenotype (Fig. 4F) were characterized as described for *hypA1* strains (Kaminskyj, 2000). Nuclei and tip cell length were characterized in fixed cells following fluorescence staining for DNA and cell walls, respectively. Tip cell viability was assessed in living cells by their ability to exclude toluidine blue. The *hypB5* strain ASK80 was grown for 13 h at 28 °C and then shifted to 42 °C. Growth temperature upshift was followed within 30 min by nuclear condensation in hyphal tip cells, then successively by nuclear fragmentation and nuclear fragment disappearance (Fig. 6). Nuclear condensation and fragmentation was temporally associated with deposition of septa within the tip cell, consequently reducing tip-to-first septum length (Fig. 6B, circles). Following tip cell septation, tip cells died (Fig. 5B, triangles) associated with nucleus fragmentation and disappearance. However, the unbranched basal cells remained alive, began to swell and their nuclei proliferated (Fig. 4F). By 3 h after upshift, unbranched *hypB5* basal cells were significantly wider than the tip cells (Fig. 4F and data not shown). When the morphological wildtype mutagenesis parent strain A28 was shifted in growth temperature from 28 °C to 42 °C there was no subsequent effect on tip cell nuclear stability, septation or viability.

4. Discussion

Aspergillus nidulans hypB was cloned by complementing the *hypB5* temperature sensitive morphogenetic defect

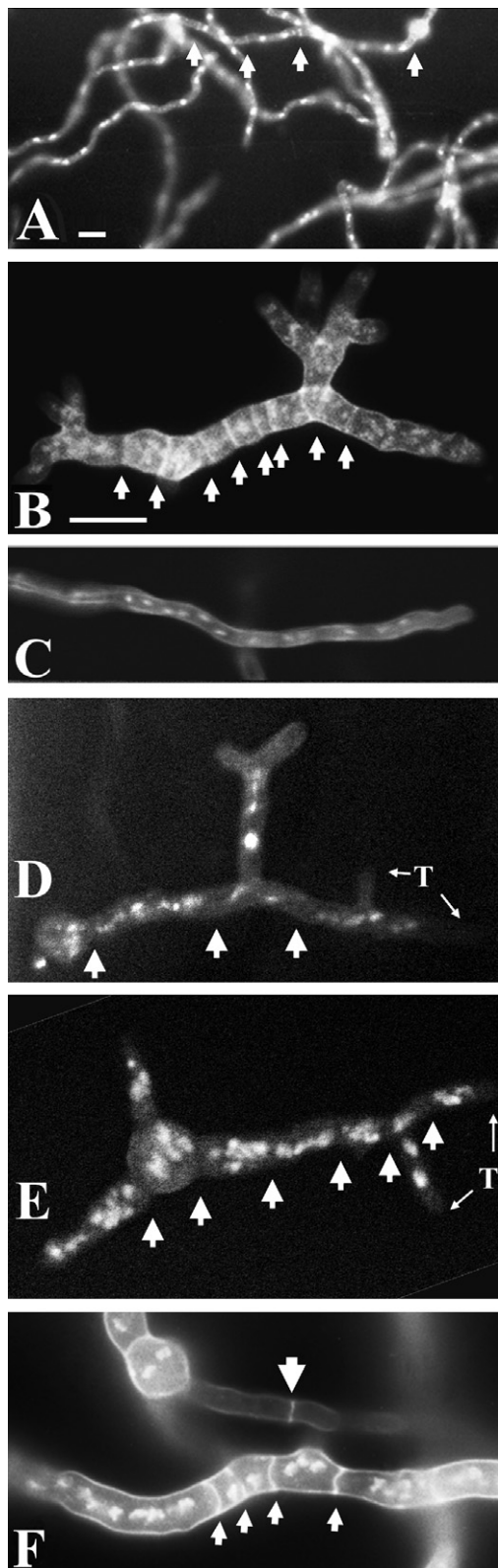


Fig. 4. Phenotypes of *Aspergillus nidulans* germlings, stained with Calcofluor and (or) Hoechst 33258 to visualize walls and nuclei, respectively. Bars = 10 μ m (in B for B–F). Arrows indicate positions of septa. Hyphae of the *hypB5* strain ASK80 grown at for 16 h at (A) 28 °C and (B) 42 °C, visualized with widefield epifluorescence. At 28 °C, *hypB5* strains hyphae resemble wildtype. At 42 °C, *hypB5* hyphae are about twice as wide as when grown at 28 °C, and have nearapical septa and abundant nuclei. (C) A *hypB5*-complemented AYY1 hypha grown at 39 °C for 16 h, visualized with confocal microscopy. AYY1 hyphae resemble wildtype strains at all growth temperatures. AN6709 Δ germling grown for 16 h at 28 °C (D) and 42 °C (E) on selective medium overlaid with dialysis tubing, stained for nuclei, and visualized with confocal microscopy. T (and associated arrows) indicates tips that were readily visible on the associated transmitted light image. Septum positions (arrows) were identified from the transmitted light image. (F) An ASK80 hypha that had been grown at 28 °C for 12 h and then shifted to 42 °C for 3 h. Within an hour of the temperature shift, nuclei in tip cells (upper hypha) suffered a lethal fragmentation that triggered septum formation, and then the tip cells died. Meanwhile, the basal cells (lower hypha) initiated growth, becoming significantly wider than the tip cells.

Table 2
Cellular characteristics^a of *Aspergillus nidulans* wildtype and *hypB5* strains

	Hyphal width $\mu\text{m} \pm \text{SE}$	Basal cell length $\mu\text{m} \pm \text{SE}$	Nuclei/basal cell mean \pm SE
A28 (39 °C) ^b	3.4 \pm 0.1 ^e	29.3 \pm 1.6 ^e	3.6 \pm 0.2 ^e
ASK 80 (<i>hypB5</i> , 39 °C) ^b	5.4 \pm 0.1 ^f	6.3 \pm 0.4 ^f	5.3 \pm 0.5 ^f
ASK166 (<i>hypB5</i> , 39 °C) ^b	5.4 \pm 0.1 ^f	6.2 \pm 0.4 ^f	5.2 \pm 0.5 ^f
AYY1 (<i>hypB5</i> -complemented, 39 °C) ^c	3.2 \pm 0.1 ^e	24.1 \pm 2.7 ^e	3.9 \pm 0.3 ^e
AN6709 Δ (28 °C) ^d	5.1 \pm 0.1 ^f	10.7 \pm 1.6 ^g	5.9 \pm 1.2 ^f

^a See Section 2 for morphometry procedures. Cells were grown about 24 h following inoculation to allow for the formation of two or more basal cells per hypha. Values in each column followed by different letters (e–g) were significantly different ($P < 0.05$, ANOVA).

^b See Table 1 and Fig. 4 for details.

^c Strain ASK166 complemented with *hypB*⁺.

^d See Fig. 2 for details.

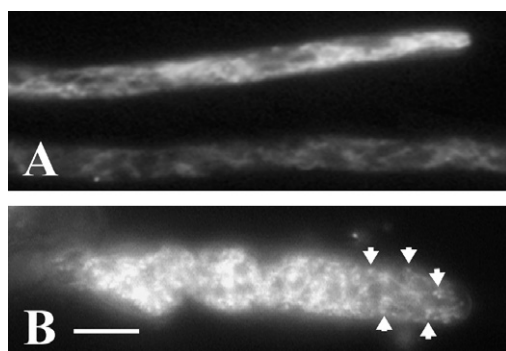


Fig. 5. Endomembranes in permissive and restrictive *hypB5* phenotype cells, visualized with FM4-64 and wildtype epifluorescence microscopy. (A) Permissive and (B) restrictive phenotype cells, that had been allowed to accumulate FM4-64 for 45 min, visualized with widefield fluorescence. Arrows indicate punctate FM4-64 accumulations in the restrictive phenotype, consistent with putative fungal Golgi, as well as considerable punctate or reticulate pattern staining in subapical regions. Bar in B = 5 μm , for A and B.

(Kaminskyj and Hamer, 1998) with the Oshero and May (2000) genomic plasmid library. A 5 kb KpnI fragment of the complementing plasmid, cloned into pYY2, could rescue the *hypB5* temperature sensitive defect, presumably by gene conversion. The pYY2 insert begins 34 bp upstream of the predicted translation start for predicted gene AN6709.4, and is identical to the N-terminal 4763 bp, except for a single bp. The terminal defect can also be rescued by AN6709 amplified by PCR from wildtype *A. nidulans* genomic DNA template. Deleting AN6709 causes hyphal morphology defects that are highly similar to the *hypB5* restrictive phenotype but are seen at the *hypB5* permissive temperature. Compared to the wildtype sequence, the predicted Sec7p domain of the *hypB5* allele had a single base pair mutation that would cause a non-conservative amino acid change, alanine to proline, in a conserved region of the translated product. Taken together, these data suggest that *A. nidulans hypB* is predicted gene AN6709.

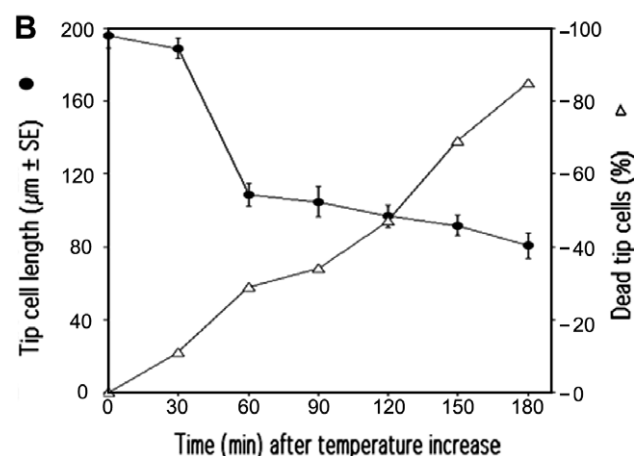
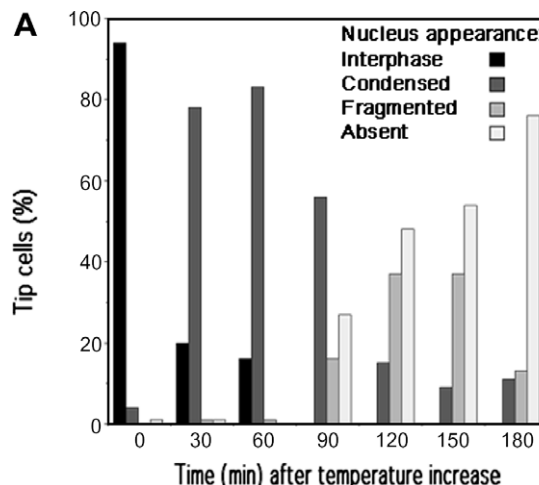


Fig. 6. Effect of a growth temperature shift from 28 °C to 42 °C on (A) tip cell nuclei and (B) septation and cell survival in an *Aspergillus nidulans hypB5* strain. Germlings were grown for 13 h at 28 °C so they had at least one septum, then were shifted to 42 °C. (A) Hyphal tip cell nucleus appearance in Hoechst 33258-stained hyphae was characterized as interphase (black bars), condensed (dark grey bars), fragmented (light grey bars) or lacking (pale grey bars). (B) Tip to first septum distance (filled circles) was measured in Calcofluor stained hyphae. Cell viability, expressed as % dead cells (open triangles) was assessed in unfixed cells by their ability to exclude toluidine blue. Three sets of 100 Calcofluor-stained cells were assessed for tip-to-first septum spacing; 100 cells were assessed for membrane integrity. Tip-to-first septum (tip cell length) reduction, indicating insertion of one or more septa, correlated with nuclear condensation (shown in A). Tip cell death correlated with nuclear fragmentation and loss (shown in A).

The *hypB* locus was originally assigned to chromosome VII by mitotic mapping (Kaminskyj and Hamer, 1998). However, we were not able to confirm this by meiotic mapping with chromosome VII markers. AN6709 is located on chromosome I. Given the relative uncertainty of mitotic mapping (see the result for *hypD3* in Kaminskyj and Hamer, 1998) compared to the unequivocal match between pYY2 and AN6709, supported by the AN6709 deletion and phenotype rescue results, we feel confident of the chromosome I assignment.

hypB is predicted to encode an ARF-GEF (ADP ribosylation factor guanine nucleotide exchange factor;

Chardin et al., 1996). GEFs are required in the activity cycle of small Gproteins, such as ARFs (Jackson and Casanova, 2000). The ARF protein family has three classes, variously involved in exocytosis, endocytosis and actin dynamics at the plasma membrane (Cox et al., 2004; Donaldson and Honda, 2005). Multiple ARFs and GEFs are (or are predicted to be) present in fungi (Cox et al., 2004) including *A. nidulans*. These are implicated in diverse aspects of Golgi function in metazoans (Franco et al., 1998; Zhang et al., 1994). *A. nidulans* Golgi function has been shown to be important in hyphal morphogenesis (Shi et al., 2004; Whittaker et al., 1999).

In the COPI secretion pathway, vesicle formation depends on Arf1 binding to the donor membrane, which in turn induces vesicle coat assembly by recruiting cytosolic coat proteins to reshape the donor membrane into a sphere (Gaynor et al., 1998). When Arf1 binds GTP, which requires a GEF, a conformational change exposes an N-terminally bound myristate that inserts into the membrane to initiate coat assembly. GEF activity resides in the Sec7 domain, which is sufficient for activity (Chardin et al., 1996; Jackson and Casanova, 2000; Mossessova et al., 1998). It seems likely that *hypB*^{Sec7} will interact with a myristoylation factor such as *swoF* (Shaw et al., 2002). Attempts to produce a *hypB*, *swoF* double mutant strain using genetic techniques (Kaminskyj, 2001) have been unsuccessful. Cleistothecia formed, but of more than 25 that were analyzed, all were self-crossed or their ascospores were unviable, the latter suggesting there may be a deleterious interaction between the *hypB* and *swoF* mutants.

The Sec7p domain appears to be important for HypB function. Sec7p domains have 10 alpha helices, A–J, of which F–H form the nucleotide binding site (Cherfils et al., 1998). The loop between helix F and G is highly conserved and is reported to be important for nucleotide binding (Cherfils et al., 1998). The *hypB5* allele has a non-conservative amino acid change (A815P) in helix F of its predicted Sec7p domain. In a model polyaniline helix, substituting one proline decreased stability by 3.16 kJ/mol, compared to about 1 kJ/mol for the next most destabilizing amino acid change (Pace and Scholtz, 1998). The A815P mutation is expected to affect the affinity of the nucleotide binding site in the *hypB5* gene product, likely accounting for the marked temperature sensitivity of *hypB5* mutant strains as well as their mild permissive phenotype (Kaminskyj and Hamer, 1998). Taken together, these data strongly suggest that AN6709 is *hypB*^{Sec7}.

Fungal growth requires production and targeted fusion of wall building vesicles with the apical plasma membrane (Bartnicki-Garcia, 2002). Golgi bodies modify, sort, and package components for diverse destinations (Matheson et al., 2006). Transmission electron microscopy shows that metazoan and plant Golgi are composed of stacks of cisternae, whereas *A. nidulans* Golgi, like other fungi, are single cisternae (Kaminskyj and Boire, 2004; Kurtz et al., 1994). Vesicle formation employs membrane-associated protein skeletons, which in fungi are composed of coatomer pro-

tein assemblies called COPI and COPII (Barlowe et al., 1994; Bednarek et al., 1995; Haucke, 2003; Serafini et al., 1991). COPI-coated vesicles, associated with Golgi to ER (retrograde) traffic, interact with the conserved oligomeric Golgi (COG) (Ungar et al., 2002) complex, whereas COPII-coated vesicles, associated with anterograde traffic, interact with the transport protein particle (TRAPP) complex (Cai et al., 2005). Models describing Golgi transport include the vesicular transport model and the cisternal maturation model, reviewed in Ungar et al. (2006). In both models, COPII-coated vesicles mediate anterograde ER–Golgi transport and Golgi exit, and COPI coated vesicles mediate membrane and protein retrieval (Guo et al., 2000). The vesicular transport model proposes that both anterograde and retrograde Golgi traffic is vesicle mediated, whereas the cisternal maturation model posits that most vesicular traffic is retrograde. Another subunit in the COPI pathway is *A. nidulans sod*^{VTC}, predicted to encode alpha-COPI (Whittaker et al., 1999; Breakspear et al., 2007). *A. nidulans hypA*^{TRSI20} is homologous to *S. cerevisiae* Trs120p, a regulatory associate of TRAPP II. It is likely that *A. nidulans* endomembrane trafficking will be similarly regulated to that of *S. cerevisiae*.

Endomembranes visualized by FM4-64 staining differed between the permissive and restrictive *hypB5* phenotypes. The permissive phenotype was consistent with wildtype patterns (Shi et al., 2004). Even wildtype phenotype *A. nidulans* hyphae can vary tremendously in growth rate (Hubbard and Kaminskyj, 2007), and it is not always possible to see an apical FM4-64 accumulation. In contrast, the *hypB5* restrictive phenotype had prominent stain accumulation in punctate and reticulate arrays. These likely represent fungal Golgi and ER. Growth rate of the *hypB5* restrictive phenotype is substantially reduced compared to permissive (Kaminskyj and Hamer, 1998), which is consistent with the relative lack of apical staining.

Aspergillus nidulans hypB^{Sec7p} is not essential, since conidia from the AN6709Δ transformants sporulated readily, and those spores germinated on selective medium (Nayak et al., 2006). Diagnostic PCR showed that AN6709Δ mycelium amplified the expected size band using primers from the flanking region and, in particular, primers designed to amplify a chimaeric sequence containing the *AFpyrG* selectable marker and the 3' untranslated region amplified a strong band. In each case, these were distinctly different results from PCRs with the same primers but using genomic template from the A1145 parent strain. The AN6709Δ phenotype closely resembles the *hypB5* restrictive phenotype regarding hyphal width, branch frequency and branching angle, but does so at the *hypB5* permissive temperature.

There were differences between the *hypB5* restrictive phenotype and the AN6709Δ phenotype regarding basal cell length and nucleus abundance: AN6709Δ germlings grown at 28 °C had more uneven hyphal width and fewer septa, and in addition when grown at 42 °C, AN6709Δ germlings had relatively abundant nuclei and more closely

spaced septa. Like the *hypB5* restrictive phenotype, AN6709 Δ cells were branched in near-apical regions. Differences with respect to the temperature sensitive conditional phenotype may relate to the AN6709 Δ strain lacking all of *hypB*^{Sec7}, rather than having a defective Sec7p domain in an otherwise intact gene product. Similarly, the *hypA1* temperature sensitive mutant had a related but distinct restrictive phenotype compared to the *hypA* deletion strain (Shi et al., 2004).

Both *A. nidulans hypA* and *hypB* affect hyphal morphogenesis and coordination between growth and cell cycle progression. In *hypA1* strains grown at 28 °C and shifted to 42 °C, nuclei in tip cells suffered a lethal nuclear division that triggered deposition of regularly-spaced septa (Kaminskyj, 2000). The time course of phenotype changes in *hypB5* strains following growth temperature upshift was similar to that of *hypA1*, and both have the same terminal phenotype. However, these are independent genes predicted to function in different endomembrane pathways. Thus, *A. nidulans* cell growth controls appear to use multifaceted regulatory inputs, and *A. nidulans* gene products appear to play multiple cellular roles.

We have shown that the *A. nidulans hypB5* encodes a Sec7-domain protein, predicted gene AN6709 in the *A. nidulans* genome database, and that this domain is important for wildtype function. Sec7-domain proteins are nucleotide exchange factors for small G-proteins, including ARFs, which play a critical role in an early stage of vesicle formation consistent with the morphological and endomembrane abnormalities in the *hypB5* restrictive phenotype. The *hypB5* upshift phenotype shows that like *hypA*^{Trs120}, *hypB*^{Sec7} has a role in coordinating cell growth and the nuclear cycle.

Acknowledgments

This work was supported by funding from the Natural Sciences and Engineering Research Council of Canada (S.G.W.K., D.A.R.S.), and postgraduate scholarships from the University of Saskatchewan (Y.Y.), and the Egyptian Ministry of Higher Learning (A.E.). We thank Christine Jaspas for characterizing the *hypB5* upshift phenotype.

References

- Barlowe, C., Orci, L., Yeung, T., Hosobuchi, M., Hamamoto, S., Salama, N., Rexach, M.F., Ravazzola, M., Amherdt, M., Schekman, R., 1994. COPII: A membrane coat formed by SEC proteins that drive vesicle budding from the endoplasmic reticulum. *Cell* 77, 895–907.
- Bartnicki-Garcia, S., 2002. Hyphal tip growth: outstanding questions. In: Osiewicz, H.D. (Ed.), *Molecular Biology of Fungal Development*. Marcel Dekker, New York, pp. 29–58.
- Bednarek, S.Y., Ravazzoala, M., Hosobuchi, M., Amherdt, M., Perrelet, A., Schekman, R., Orci, L., 1995. COPI- and COPII-coated vesicles bud directly from the endoplasmic reticulum in yeast. *Cell* 83, 1183–1196.
- Breakspear, A., Langford, K.J., Momany, M., Assinder, S.J., 2007. CopA:GFP localizes to putative Golgi equivalents in *Aspergillus nidulans*. FEMS Microbiol. Lett. FEMS Microbiol. Lett. Online: 19Oct2007; doi:10.1111/j.1574-6968.2007.00945.x.
- Cai, H., Zhang, Y., Pypaert, M., Walker, L., Ferro-Novick, S., 2005. Mutants in *trsl20* disrupt traffic from the early endosome to the late Golgi. *J. Cell Biol.* 171, 823–833.
- Chardin, P., Paris, S., Antonny, B., Robineau, S., Beraud-Dufour, S., Jackson, C.L., Chabre, M., 1996. A human exchange factor for ARF contains Sec7- and pleckstrin-homology domains. *Nature* 384, 481–484.
- Cherfils, J., Menetrey, J., Mathieu, M., La Bras, G., Robineau, S., Beraud-Dufour, S., Antonny, B., Chardin, P., 1998. Structure of the Sec7 domain of the ARF exchange factor ARNO. *Nature* 392, 101–105.
- Cox, R., Mason-Gamer, R.J., Jackson, C.L., Segev, N., 2004. Phylogenetic analysis of Sec7domain-containing ARF nucleotide exchangers. *Mol. Biol. Cell* 15, 1487–1505.
- Donaldson, J.G., Honda, H., 2005. Localization and function of Arf family GTPases. *Biochem. Soc. Trans.* 33, 639–642.
- Franco, M., Boretto, J., Robineau, S., Monier, S., Goud, B., Chardin, P., Chavrier, P., 1998. ARNO3, a Sec7-domain guanine nucleotide exchange factor for ADP ribosylation factor 1, is involved in the control of Golgi structure and function. *Proc. Natl. Acad. Sci. USA* 95, 9926–9931.
- Gaynor, E.C., Graham, T.R., Emr, S.D., 1998. COPI in ER. *Biochim. Biophys. Acta-Mol. Cell Res.* 1404, 33–51.
- Guo, W., Sacher, M., Barrowman, J., Ferro-Novick, S., Novick, P., 2000. Protein complexes in transport vesicle targeting. *Trends Cell Biol.* 10, 251–255.
- Hamer, L., Adachi, K., Montenegro-Chamorro, M.V., Tanzer, M.M., Mahanty, S.K., Lo, C., Tarpey, R.W., Skalchunes, A.R., Heiniger, R.W., Frank, S.A., Darveau, B.A., Lampe, D.J., Slater, T.M., Ramamurthy, L., DeZwaan, T.M., Nelson, G.H., Shuster, J.R., Woessner, J., Hamer, J.E., 2001. Gene discovery and gene function assignment in filamentous fungi. *Proc. Natl. Acad. Sci. USA* 98, 5110–5115.
- Harris, S.D., 2006. Cell polarity in filamentous fungi: shaping the mold. *Intl. Rev. Cytol.* 251, 41–77.
- Harris, S.D., Hoffman, A.F., Tedford, H.W., Lee, M.P., 1999. Identification and characterization of genes required for hyphal morphogenesis in the filamentous fungus *Aspergillus nidulans*. *Genetics* 151, 1015–1025.
- Harris, S.D., Momany, M., 2004. Polarity in filamentous fungi: Moving beyond the yeast paradigm. *Fung. Genet. Biol.* 41, 391–400.
- Harris, S.D., Morrell, J.L., Hamer, J.E., 1994. Identification and characterization of *Aspergillus nidulans* mutants defective in cytokinesis. *Genetics* 136, 517–532.
- Harris, S.D., Read, N.D., Roberson, R.W., Shaw, B.D., Seiler, S., Plamann, M., Momany, M., 2005. Polarisome meets Spitzenkörper: microscopy, genetics, and genomics converge. *Euk. Cell* 4, 225–229.
- Hauke, V., 2003. Vesicle budding: A coat for the COPs. *Trends Cell Biol.* 13, 59–60.
- Hill, T.W., Loprete, D.M., Momany, M., Ha, Y., Harsch, L.M., Livesay, J.A., Mirchandani, A., Murdock, J.J., Vaughan, M.J., Watt, M.B., 2006. Isolation of cell wall mutants in *Aspergillus nidulans* by screening for hypersensitivity to Calcofluor white. *Mycologia* 98, 399–409.
- Hubbard, M., Kaminskyj, S., 2007. Growth rate of *Aspergillus nidulans* hyphae is largely independent of cytoplasmic microtubule abundance. *Mycol. Prog.* 6, 179–189.
- Jackson, C.L., Casanova, J.E., 2000. Turning on ARF: the Sec7 family of guanine nucleotide-exchange factors. *Trends Cell Biol.* 10, 60–67.
- Kaminskyj, S.G.W., 2000. Septum position is marked at the tip of *Aspergillus nidulans* hyphae. *Fung. Genet. Biol.* 31, 105–113.
- Kaminskyj, S.G.W., 2001. Fundamentals of growth, storage, genetics and microscopy of *Aspergillus nidulans*. *Fung. Genet. Newsl.* 48, 25–31.
- Kaminskyj, S.G.W., Boire, M.R., 2004. Ultrastructure of the *Aspergillus nidulans hypA1* restrictive phenotype shows defects in endomembrane arrays and polarized wall deposition. *Can. J. Bot.* 82, 807–814.

- Kaminskyj, S.G.W., Hamer, J.E., 1998. *hyp* Loci control cell pattern formation in the vegetative mycelium of *Aspergillus nidulans*. *Genetics* 148, 669–680.
- Kim, Y., Raunser, S., Munger, C., Wagner, J., Song, Y., Cygler, M., Walz, T., Oh, B., Sacher, M., 2006. The architecture of the multisubunit TRAPP I complex suggests a model for vesicle tethering. *Cell* 127, 817–830.
- Kurtz, M.B., Heath, I.B., Marrinan, J., Dreikorn, S., Onishi, J., Douglas, C., 1994. Morphological effects of lipopeptides against *Aspergillus fumigatus* correlate with activities against (1,3)- β -D-glucanase. *Antimicrob. Agents Chemother.* 38, 1480–1489.
- Lin, X., Momany, C., Momany, M., 2003. SwoHp, a nucleoside diphosphate kinase, is essential in *Aspergillus nidulans*. *Euk. Cell* 2, 1169–1177.
- Matheson, L.A., Hanton, S.L., Brandizzi, F., 2006. Traffic between the plant endoplasmic reticulum and the Golgi apparatus: to the Golgi and beyond. *Curr. Opt. Cell Biol.* 9, 601–609.
- Momany, M., Westfall, P.J., Abramowsky, G., 1999. *Aspergillus nidulans swo* mutants show defects in polarity establishment, polarity maintenance and hyphal morphogenesis. *Genetics* 151, 556–567.
- Mossessova, E., Gulbis, J.M., Goldberg, J., 1998. Structure of the guanine nucleotide exchange factor Sec7 domain of human ARNO and analysis of the interaction with ARF GTPase. *Cell* 92, 415–423.
- Nayak, T., Szewczyk, E., Oakley, C.E., Osmani, A., Ukil, L., Murray, S.L., Hynes, M.J., Osmani, S.A., Oakley, B.R., 2006. A versatile and efficient gene-targeting system for *Aspergillus nidulans*. *Genetics* 172, 1557–1566.
- Oshero, N., Mathew, J., May, G.S., 2000. Polarity-defective mutants of *Aspergillus nidulans*. *Fung. Genet. Biol.* 31, 181–188.
- Oshero, N., May, G., 2000. Conidial germination in *Aspergillus nidulans* requires RAS signaling and protein synthesis. *Genetics* 155, 647–656.
- Pace, C.N., Scholtz, J.M., 1998. A helix propensity scale based on experimental studies of peptides and proteins. *Biophys. J.* 75, 422–427.
- Sáli, A., Blundell, T.L., 1993. Comparative protein modelling by satisfaction of spatial restraints. *J. Mol. Biol.* 234, 779–815.
- Serafini, T., Stenbeck, G., Brecht, A., Lottspeich, F., Orci, L., Rothman, J.E., Wieland, F.T., 1991. A coat subunit of Golgi-derived non-clathrin-coated vesicles with homology to the clathrin-coated vesicle coat protein beta-adaptin. *Nature* 349, 215–220.
- Sharpless, K.E., Harris, S.D., 2002. Functional characterization and localization of the *Aspergillus nidulans* formin SEPA. *Mol. Biol. Cell* 13, 469–479.
- Shaw, B.D., Momany, C., Momany, M., 2002. *Aspergillus nidulans swoF* encodes an N-myristoyl transferase. *Euk. Cell* 1, 241–248.
- Shi, X., Sha, Y., Kaminskyj, S., 2004. *Aspergillus nidulans hypA* regulates morphogenesis through the secretion pathway. *Fung. Genet. Biol.* 41, 75–88.
- Strathmann, M., Hamilton, B.A., Mayeda, C.A., Simon, M.I., Meyerowitz, E.M., Palazzolo, M.J., 1991. Transposon-facilitated DNA sequencing. *Proc. Natl. Acad. Sci. USA* 88, 1247–1250.
- Szewczyk, E., Nayak, T., Oakley, C.E., Edgerton, H., Xiong, Y., Taheri-Talesh, N., Osmani, S.A., Oakley, B.R., 2007. Fusion PCR and gene targeting in *Aspergillus nidulans*. *Nature Protocols* 1, 3111–3120.
- Ungar, D., Oka, T., Brittle, E.E., Vasile, E., Lupashin, V.V., Chatterton, J.E., Heuser, J.E., Krieger, M., Waters, M.G., 2002. Characterization of a mammalian Golgi-localized protein complex, COG, that is required for normal Golgi morphology and function. *J. Cell Biol.* 157, 405–415.
- Ungar, D., Oka, T., Krieger, M., Hughson, F.M., 2006. Retrograde transport on the COG railway. *Trends Cell Biol.* 16, 113–120.
- Virag, A., Harris, S.D., 2006. The Spitzenkörper: a molecular perspective. *Mycol. Res.* 110, 4–13.
- Whittaker, S.L., Lunness, P., Milward, K.J., Doonan, J.H., Assinder, S.J., 1999. sodVIC is an alpha-COP-related gene which is essential for establishing and maintaining polarized growth in *Aspergillus nidulans*. *Fung. Genet. Biol.* 26, 236–252.
- Yang, L., Ukil, L., Osmani, A., Nahm, F., Davies, J., De Souza, C.P.C., Dou, X., Perez-Balaguer, A., Osmani, S.A., 2004. Rapid production of gene replacement constructs and generation of a green fluorescent protein-tagged centromeric marker in *Aspergillus nidulans*. *Euk. Cell* 3, 1359–1362.
- Zhang, C., Rosenwald, A.G., Willingham, M.C., Skuntz, S., Clark, J., Kahn, R.A., 1994. Expression of a dominant allele of human ARF1 inhibits membrane traffic *in vivo*. *J. Cell Biol.* 124, 289–300.